Nanoscale

REVIEW

View Article Online
View Journal | View Issue

Cite this: *Nanoscale*, 2016, **8**, 12394

Porphyrin-loaded nanoparticles for cancer theranostics

Yiming Zhou, Xiaolong Liang and Zhifei Dai*

Received 8th November 2015,
Accepted 13th December 2015

DOI: 10.1039/c5nr07849k

www.rsc.org/nanoscale

Porphyrins have been used as pioneering theranostic agents not only for the photodynamic therapy, sonodynamic therapy and radiotherapy of cancer, but also for diagnostic fluorescence imaging, magnetic resonance imaging and photoacoustic imaging. A variety of porphyrins have been developed but very few of them have actually been employed in clinical trials due to their poor selectivity to tumorous tissue and high accumulation rates in the skin. In addition, most porphyrin molecules are hydrophobic and form aggregates in aqueous media. Nevertheless, the use of nanoparticles as porphyrin carriers shows great promise to overcome these shortcomings. Encapsulating or attaching porphyrins to nanoparticles makes them more suitable for tissue delivery because we can create materials with a conveniently specific tissue lifetime, specific targeting, immune tolerance, and hydrophilicity as well as other characteristics through rational design. In addition, various functional components (*e.g.* for targeting, imaging or therapeutic functions) can be easily introduced into a single nanoparticle platform for cancer theranostics. This review presents the current state of knowledge on porphyrin-loaded nanoparticles for the interwined imaging and therapy of cancer. The future trends and limitations of prophyrin-loaded nanoparticles are also outlined.

Introduction

Nowadays, cancer remains a great threat to human health worldwide. Due to the widespread metastasis with cancer, millions of patients die of cancer each year.[1] Early detection, accurate diagnosis and effective treatment help increase cancer survival rates and reduce suffering. Despite the enormous advances in diagnostic technologies, a substantial number of cancer patients are still diagnosed with metastasis because of the poor selectivity and sensitivity of conventional diagnostic techniques. A variety of therapeutic strategies, such as surgery, chemotherapy and radiation therapy, are widely used in clinical cancer treatment. However, systemic toxicity, drug resistance and low selectivity often lead to an unsatisfactory outcome.[2] Attacking these problems head on, developing innovative strategies to improve the cure rate and reducing the side-effects in cancer therapy are all urgently needed.

Nanoparticles have been widely used to load various diagnostic or therapeutic agents through chemical conjugation or physical entrapment to benefit from the sophisticated nanostructures and large surface area to volume ratios.[3] In addition, nanoparticles can be target delivered into tumours *via* passive accumulation and/or active-targeting approaches. In an attempt to surmount the major hurdles in the treatment of cancer, a variety of nanoparticles have been constructed for cancer diagnostics and therapeutics to achieve high-quality cancer imaging and to achieve enhanced therapeutic efficacy with nosevere cytotoxicity to normal cells.[4] In particular, theranostic nanoparticles as a treatment combining cancer diagnostic imaging and consequently targeted therapy have attracted intensive interest.[5,6] The most exciting feature of such theranostic nanoparticles for use in drug delivery is the capability to embrace multiple techniques to arrive at comprehensive diagnosis, molecular imaging and an individualized treatment regimen through imaging guidance and treatment response monitoring.[7,8] Theranostic nanotechnologies may provide patients with various treatment options that are suitable for specific individuals, which thereby result in improved prognoses.[9]

Porphyrins consist of four pyrrole subunits linked together by four methine bridges.[10] Researchers have shown great interest in porphyrin and its derivatives, not only because of their well-described photosensitizing properties but also because of their capability to selectively accumulate in tumour tissues, and to persist there for long periods of time.[11] These unique features have led to their potential use as adjuvants and sensitizers in a variety of biomedical applications, including not only diagnostic imaging (*e.g.* fluorescence imaging,[12] magnetic resonance imaging (MRI)),[12] but also therapies (*e.g.* photodynamic therapy (PDT),[13] sonodynamic therapy (SDT), boron

Department of Biomedical Engineering, College of Engineering, Peking University, Beijing 100871, China. E-mail: zhifei.dai@pku.edu.cn

neutron capture therapy (BNCT),[14] and radiation therapy (RT)).[15] PDT (or SDT) and BNCT are binary cancer therapies involving the activation of tissue-localized sensitizers with either light (in PDT), or ultrasound (in SDT) or low-energy neutrons (in BNCT). Thus, porphyrin and its related compounds can be a type of promising theranostic agent. By employing these therapeutic methodologies, we can achieve local tumor control with minimal side-effects in comparison with other cancer treatments (surgery, radiotherapy, and chemotherapy). Porphyrins constitute a major class of pharmacological agents currently under investigation. Photofrin and Visudyne, two porphyrin derivatives, have been approved in the USA as PDT drugs by the U.S. Food and Drug Administration (FDA). Nevertheless, the low aqueous solubility of porphyrin and its related compounds may limit their biomedical applications. Most porphyrins that are in use clinically or in preclinical development are hydrophobic and strongly aggregate in aqueous media. This aggregation significantly reduces their therapeutic efficacy because only monomeric species are appreciably active.[16] Although porphyrins preferentially accumulate in cancer cells probably due to the high vascular permeability of the porphyrins, their affinity for proliferating endothelium and the lack of lymphatic drainage in tumours[17] means that healthy cells also tend to uptake porphyrins in a considerable proportion. Thus, the cytotoxicity of porphyrins to healthy cells should be taken into consideration as well.

In recent years, with the rapid development of nanotechnology in the biomedical field, various types of nanoparticles, such as liposomes, polymeric micelles, inorganic and hybrid nanoparticles, have been widely used to fabricate stable aqueous dispersions of porphyrins owing to their high biocompatibility, good biodegradability and their easy modification for specific targeting.[18] The loading of porphyrins into nanoparticles could overcome the abovementioned problems. Moreover, the other diagnostic and therapeutic components could also be integrated into such porphyrin-based nanoparticles for theranostic nanomedicine.[19] In particular, the multimodality imaging functionalization of porphyrin nanotheranostic agents is of interest for the personalized monitoring of *in vivo* tumour targeting and pharmacokinetics of porphyrin nanotheranostic agents for predicting therapy outcome and gaining a better understanding of the prognosis-associated disease status by combining the advantageous information from each imaging modality.

In this review, we summarize the latest advances of porphyrin-based nanoparticles for cancer treatment, including biomedical imaging, drug delivery, therapy and combination of diagnosis and therapy. For a deeper understanding of cancer theranostics based on porphyrin nanoagents, the limitations and prospects of porphyrin nanoagents are also discussed.

Porphyrins for cancer theranostics

Porphyrins can accumulate in cancerous tissues to a higher extent than in the surrounding healthy tissues, and the ratio of tumour tissue to normal tissue is generally about 2–3 : 1, thus they are suitable for intrinsic imaging and cancer therapy. Based on the generation of reactive oxygen species (ROS) upon activation by light or ultrasound, porphyrinic molecules have been widely used as photosensitizers for the PDT or SDT of cancer. As excellent metal chelators, porphyrins are very efficient at delivering radioisotopes for radiotherapy. In addition to their therapeutic applications, porphyrins can also be labelled with radioisotopes and coupled with magnetic resonance imaging agents to provide multifunctional probes for positron emission tomography (PET) and MRI.[20–22] Moreover, porphyrins can be excited employing visible light to emit red or near-infrared fluorescence, which is useful for diagnostic fluorescence imaging to evaluate intracellular localization and treatment effects. Such intertwined imaging and therapeutic properties of porphyrins permit theranostic treatments of cancer.

To carry out PDT treatment, clinicians need to control the laser power, laser irradiation time, drug dose, and number of laser treatments. Thus, it is highly necessary to develop feedback systems to guide PDT treatment. Consequently, such theranostic porphyrins are likely to become more routinely utilized image guidance tools for the use of setting and adjusting the parameters of PDT treatments in the future.[20–25] Actually, porphyrins have already been used as pioneering theranostic agents. Besides being used for cancer PDT, heme derivatives have been used for cancer imaging as early as the 1920s, and porphyrins have been used as MRI contrast agents since the 1980s.[26] Recently, Soumya reported the use of optical imaging strategies to noninvasively examine photosensitizer distribution and physiological and host responses to 2-[1-hexyloxyethyl]-2-devinyl pyropheophorbide-a (HPPH)-mediated PDT of EMT6 tumors.[27] During SDT, cancer cells could be destructed by utilizing a novel porphyrin derivative upon irradiation with sound rather than light due to the generation of singlet oxygen.[28] SDT is more advantageous than PDT because of the superior travel ability of sound waves through body tissue compared to light waves. By combining PDT and Förster-fluorescence resonance energy transfer (FRET), Zheng *et al.* constructed photodynamic molecular beacons (PMB) comprising a porphyrin, a $^1O_2$ quencher and an apoptotic factor-cleavable linker. The photoactivity of porphyrin is silenced until the linker interacts with a tumor-associated biomarker of the matrix metalloproteinase-7 (MMP7). MMP7 could trigger PMB not only to produce $^1O_2$ for photodynamic cytotoxicity in cancer cells but also to emit strong fluorescence for the diagnostic imaging of a tumor. Thus, a highly selective porphyrin-based theranostic agent was developed for selective cancer fluorescence imaging and PDT.[29] Pandey *et al.* developed a series of porphyrin conjugates for use in combined PDT and multimodal imaging (PET, MRI or fluorescence imaging),[30] which allowed them to assess treatment outcome (pre-, during and post-PDT). By labelling HPPH with ^{124}I, a PET-active photosensitizer was demonstrated to achieve 100% tumour-free progression 60 days after PDT.[21,25] A copper porphyrin-peptide-folate (^{64}Cu-PPF) was proved to be targeted against folate receptor positive tumours and intertwined as a PET

probe for cancer imaging and as a photosensitizer for cancer PDT (Fig. 1).[31] The half-life of the radioisotope was compatible with the pharmacokinetics of porphyrins. After chelating with ^{64}Cu ion, the biodistribution properties of the porphyrin showed no change.[32] This enables the monitoring of porphyrin tumour uptake in patients during PDT by PET imaging, and facilitates the prediction and quantitative assessment of photosensitizer accumulation in tumours, as well as assists treatment planning.[31] Bacteriochlorophylls are a very attractive agent for optical imaging because near-IR wavelengths provide deeper tissue penetration.[33] Firnau *et al.* reported that a bacteriochlorophyll-peptide-folate (BPF) could elicit tumour margins well within the surgical resection bed, allowing for complete tumour resection and the intra-operative detection of small metastatic lesions. The chelation of copper ions increased the stability of bacteriochlorophyll molecules, ensuring that ^{64}CuBPF acted as an effective theranostic agent for both PET imaging and PDT.[33]

During PDT treatment, a light-induced chemical reaction can generate localized tissue damage for both cancerous and surrounding non-malignant tissues. Thus, patients should be kept away from direct sunlight or strong indoor lighting to avoid skin phototoxicity after PDT treatment. To overcome this problem, Zhu *et al.* developed a pH-activatable photosensitizer of 5,10,15,20-tetrakis(*N*-(2-(1*H*-imidazol-4-yl)ethyl)benzamide) porphyrin (TIEBAP) to achieve a highly selective accumulation of the photosensitizer in tumour cells by modifying porphyrin with imidazole-substituents. TIEBAP showed weak fluorescence because of the face-to-face aggregation of the porphyrins caused by their poor water solubility at pH 8.0. When the pH value was altered to 5.3, a strong fluorescence was observed due to an increase in the hydrophilicity. TIEBAP produced twice as many $^1O_2$ molecules at pH 5.0 than at pH 7.4, resulting in significantly enhanced photocytotoxicity in the tumour.[34]

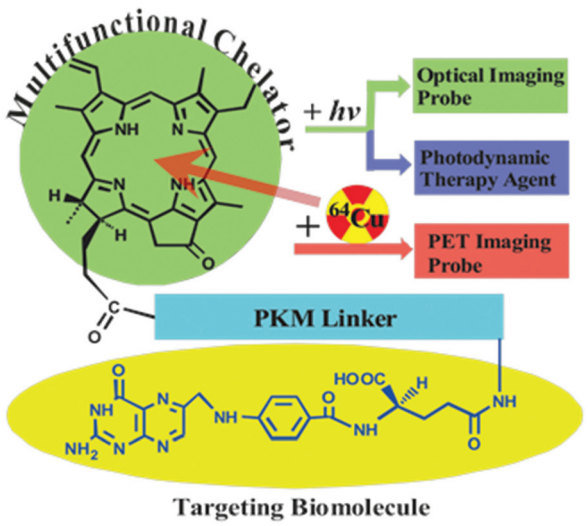

Fig. 1 The structure design of porphyrin-peptide-folate. The PKM linker is the peptide sequence, GDEVDGSGK. Reprinted with permission from ref. 31. Copyright © 2015 Ivyspring.

As an ideal photosensitizer for photodynamic theranostics, porphyrins should have good stability, a minimal self-aggregation tendency, non-toxicity in the absence of light exposure, strong absorption in the red and near-infrared region of the spectra, high target specificity and quick clearance from the body. A variety of porphyrins have been developed as PDT photosensitizing agents but few of them have been employed in clinical trials due to their poor tumor selectivity, relatively short absorption wavelengths, low extinction coefficients and high accumulation rates in the skin. In addition, most porphyrin molecules are hydrophobic and tend to form aggregates, which may result in a reduction in $^1O_2$ formation and fluorescence quantum yield. Nevertheless, the use of nanoparticles as porphyrin carriers shows great promise to overcome their shortcomings as PDT photosensitizers.

Nanoparticles for porphyrin delivery

The delivery of hydrophobic porphyrins to the target sites is one of the main challenges in PDT to be overcome. Nanoparticles are able to spontaneously accumulate in solid tumours through the enhanced permeation and retention (EPR) effect due to a combination of leaky vasculature, poor lymphatic drainage and increased vessel permeability.[35,36] Encapsulating or attaching porphyrins to nanoparticles makes them more suitable for tissue delivery, because we can create specific tissue lifetime, specific targeting, immune tolerance, and hydrophilicity, as well as other characteristics for porphyrins through rational design. Roy *et al.* entrapped chlorin of 2-devinyl-2-(1-hexyloxyethyl) pyropheophorbide into organically modified silica-based nanoparticles. The resulting monodisperse, stable nanoparticles showed higher fluorescence in an aqueous solution in comparison with the free drug, and an efficient uptake by tumour cells *in vitro* and thereby significant cell death after light irradiation.[37] Huang *et al.* developed a novel theranostic platform based on chlorin e6 (Ce6)-conjugated carbon dots with excellent tumor-homing ability for the near-infrared fluorescence imaging-guided PDT treatment of gastric cancer tumours *in vivo*.[38]

Nanoparticles provide potential to combine PDT with other therapies (*e.g.* radiotherapy and hyperthermia). Chen *et al.* covalently attached porphyrins to several doped nanoparticles (LaF_3:Ce^{3+}, LuF_3:Ce^{3+}, CaF_2:Mn^{2+}, CaF_2:Eu^{2+}, BaFBr:Eu^{2+}, BaFBr:Mn^{2+}, and $CaPO_4$:Mn^{2+}) and semiconductor nanoparticles (ZnO, ZnS, and TiO_2). Upon exposure to ionizing radiations such as X-rays, the nanoparticles emit scintillation or persistent luminescence, which activates the photosensitizers to generate $^1O_2$. This modality will provide an efficient approach to PDT while still offering the benefits of augmented radiation therapy at lower doses with no need for light delivery to the photosensitizer. In addition, radiotherapy and PDT are activated in combination by a single source, resulting in a simpler technique than either PDT used alone or both therapies used simultaneously.[15] Hyperthermia therapy has been applied to augment the efficacy of various cancer treatments.

By conjugating porphyrin molecules onto iron oxide nanoparticles, a combination treatment with both PDT and hyperthermia therapies was obtained.[39,40] Indeed, hyperthermia therapy has been found to be able to enhance the cellular uptake of oxygen molecules.[41] Moreover, magnetic iron oxide nanoparticles have excellent capability to enhance MRI imaging. Therefore, porphyrin-decorated iron oxide nanoparticles show potential for cancer theranostic applications.

Although a variety of structurally stable inorganic nanoparticles have been investigated for porphyrin delivery, their disadvantages are their inherent non-biodegradability, high rigidity and mass density, as well as low biocompatibility, which may limit their potential clinical applications. Ideal nanoparticles to deliver porphyrins for cancer theranostics should possess the following characteristics: (1) no toxicity and minimum immunogenicity, (2) good biodegradability; (3) selective accumulation of porphyrins within the diseased tissue in therapeutic concentrations with little or no uptake by non-target cells,[42] (4) high drug encapsulation efficiency (>80%) and high drug loading content (>30%), (5) capability to cross biological barriers, (6) no loss or alteration of porphyrin's activity, (7) prolonged blood circulation and minimal self-aggregation tendency, by providing an environment where porphyrins can be administered in monomeric form and (8) higher photostability than free porphyrins for *in vivo* applications.

Polymeric nanoparticles have attracted intensive attention as possible means of delivering porphyrins due to their main advantages, including good biocompatibility and biodegradability, high drug loading, controlled drug release and the ability to utilize various materials and fabrication processes. The chemical composition and architecture of polymers may be conveniently designed to load porphyrins with variable hydrophobicity, molecular weight and charge. Moreover, the biodistribution and release kinetics of porphyrin photosensitizers can be easily optimized by the surface properties, morphologies, composition and degradation of polymer matrices. Using the technique of emulsification-diffusion, p-THPP was entrapped into biodegradable nanoparticles (<150 nm) from poly(D,L-lactide-*co*-glycolide) (PLGA) and poly(D,L-lactide (PLA) with a drug loading of up to 7% (m/m).[43,44] Compared with free porphyrins, the porphyrin therapeutic index was improved greatly by nanoencapsulation due to satisfactory photocytotoxicity, even at a low drug concentration of 3 μg ml^{-1}. This enables reduction in the doses of porphyrin to reach the desired therapeutic effect, and thus diminishes the side-effects attributed to the diffusion of porphyrin into normal tissues.[45] Using the salting-out technique, two types of verteporfin-loaded PLGA nanoparticles with different diameters (167 and 370 nm) but the same drug loading (7%) were fabricated. Upon the incubation of EMT-6 mammary tumour cells with 70 ng ml^{-1} of free or big verteporfin-loaded nanoparticles, only 11% and 29% reductions in cell viability were induced, respectively. On the contrary, the small verteporfin-loaded nanoparticles provided almost 69% reduction in cell viability at the same concentration of the drug. The small-sized nanoparticles could improve the photocytotoxic efficiency of verteporfin due to effective drug delivery to the tumour and relatively higher intracellular uptake in comparison to both large-sized nanoparticles and the aqueous solution. The *in vivo* experiment showed that small verteporfin encapsulated nanoparticles could effectively inhibit tumour growth for 20 days in mice.[46]

A main shortcoming of nanoparticles is their uptake by the macrophages and accumulation in the spleen and the liver after intravenous administration. Coating with poly(ethylene glycol) (PEG) can prolong the blood circulation time of nanoparticles, and subsequently increase accumulation in tumors. Dai *et al.* successfully fabricated a theranostic agent by the formation of a Au nanoshell around poly(lactic acid) nanoparticles entrapping doxorubicin, followed by linking a Mn–porphyrin derivative on the Au shell surface through polyethylene glycol. The resulting agent exhibited excellent colloidal stability and a long blood circulation time due to the introduction of polyethylene glycol. Grafting Mn–porphyrin onto the nanoparticle surface provided a greatly improved relaxivity (r_1 value of 22.18 mM^{-1} s^{-1} of Mn^{3+}), favourable for accurate cancer diagnosis and locating the tumour site to guide the external near-infrared laser irradiation for the photothermal ablation of tumours. It was proven that the combination of chemotherapy and photothermal therapy through such a theranostic agent offered a synergistically improved therapeutic outcome compared with either therapy alone, making it a promising approach for cancer therapy.[47] It was reported that the encapsulation of protoporphyrin IX in methoxy poly(ethylene glycol)-*b*-poly(caprolactone) micelles resulted in a great enhancement in photodynamic therapy efficiency due to higher intracellular accumulation and stronger photocytotoxicity of the encapsulated protoporphyrin IX in comparison to the free drug.[48] Likewise, PEG-modified dendrimers, including poly(amido amine) and poly(propylene imine), were found to be able to deliver protoporphyrin IX to mitochondria, resulting in higher fluorescent quantum yields and more efficient cytotoxicity than the free protoporphyrin IX.[49] Chen *et al.* developed a multifunctional theranostic platform based on Ce6-loaded plasmonic vesicular assemblies of gold nanoparticles (GNPs) with PEG coating (Fig. 2). The resulting Ce6-loaded GVs (GV-Ce6) were demonstrated to show a high Ce6 loading efficiency of 18.4 wt%, an enhanced cellular uptake efficiency of Ce6 and strong NIR absorption, enabling trimodality NIR fluorescence/thermal/photoacoustic imaging-guided synergistic photothermal/photodynamic therapy (PTT/PDT) with improved efficacy using single wavelength continuous wave laser irradiation.[50]

A more direct and specific localization of a photosensitizer of porphyrins with increased efficiency and selectivity can be achieved by active targeting. This strategy relies on the attachment of a receptor-targeting moiety to the porphyrin-loaded nanoparticles, which can enhance the affinity of the binding moiety to the receptor or antigen on the targeted cell surface, allowing for a lower effective dose of the PDT photosensitizer of porphyrins. Cui *et al.* fabricated a folic acid-conjugated

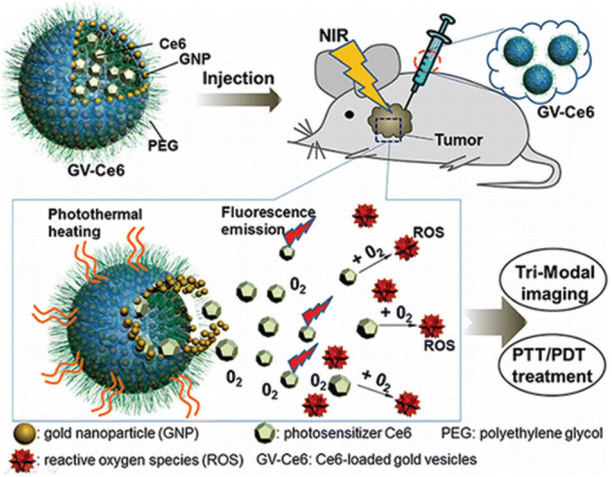

Fig. 2 Photosensitizer (Ce6)-loaded plasmonic gold vesicles (GVs) for trimodality fluorescence/thermal/photoacoustic imaging-guided synergistic photothermal/photodynamic cancer therapy. Reprinted with permission from ref. 50. Copyright © 2013 American Chemical Society.

graphene oxide (GO) for effectively loading chlorin e6 *via* hydrophobic interactions and π–π stacking. It was found that the accumulation of chlorin e6 was significantly increased in the tumour, leading to a remarkable photodynamic efficacy on MGC803 cells upon irradiation.[51] By encapsulating chlorin into silica nanoparticles followed by targeting modification with a peptide, Benachour *et al.* developed a theranostic nanoparticle for both magnetic resonance imaging and the efficient PDT of brain cancer.[52]

For smart cancer PDT treatments, *meta*-tetra(hydroxyphenyl) chlorin (*m*-THPC) was successfully incorporated into pH-sensitive micelles based on poly(2-ethyl-2-oxazoline)-*b*-poly(D,L-lactide) diblock copolymer. Such pH-sensitive micelles were observed to more effectively release the porphyrin photosensitizer at pH 5.0 than at pH 7.4. PDT with *m*-THPC-loaded micelles had no significant adverse effects on the body weight of mice *in vivo*. In addition, after an extended delivery time, *m*-THPC-loaded micelles and free *m*-THPC showed similar antitumor effects, but the *m*-THPC-loaded micelles exhibited less skin phototoxicity *in vivo*.[53] Thus, this strategy could be used as a potential nanocarrier for PDT-mediated cancer therapy. Li *et al.* prepared a pH-activatable smart nanoparticle by adsorbing a cationic photosensitizer of *meso*-tetra(*N*-methyl-4-pyridyl) porphine onto the surface of negatively charged SiO_2 nanoparticles *via* electrostatic interactions. In an acidic solution, the attached porphyrin molecules could be separated from the surface of the silica nanoparticles because the surface charge became less negative *via* the protonation of silanol protons with decreasing pH value. This led to increased fluorescence and singlet oxygen generation, thus an improvement in fluorescence imaging and the PDT efficacy of cancer.[54] Recently, researchers have been paying more attention to deep PDT treatments of cancer by integrating porphyrins and various antenna nanoparticles.[55]

Liposomal porphyrins for cancer theranostics

As a typical nanocarrier of porphyrins, liposomes have been of particular interest in cancer PDT treatments due to their flexible accommodation, appropriate retention of drugs and rapid accumulation/release characteristics in tumour cells. It has been proven that the PDT efficacy and safety of porphyrins can be substantially improved using liposomal formulations compared to non-liposomal photosensitizers under identical conditions. Photofrin is a complex mixture of hydrophobic dimers and oligomers ranging from 2 to 9 porphyrin units primarily linked by ether bonds. After loading into liposomes, the resulting liposomal photofrin was more efficient against a human glioma implanted in rat brain than non-liposomal photofrin due to the significantly enhanced uptake of liposomal photofrin in the tumour tissue.[56] Liposome-bound haematoporphyrin or haematoporphyrin dimethylester was demonstrated to accumulate intracellularly in a twice larger amount than water-dissolved haematoporphyrin, providing a more efficient singlet oxygen generation upon irradiation.[57] Early and extensive endocytoplasmic damage was induced by liposomal porphyrins, resulting in vesiculation and mitochondria swelling. In contrast, water-soluble haematoporphyrin mainly induced damage in the plasma membrane. The different patterns of cell photodamage can be attributed to the different subcellular distribution of porphyrin molecules.[57,58] Sadzuka *et al.* examined the best conditions for liposomalization of Zn-complexed coproporphyrin I (ZnCPI) as a PDT photosensitizer. It was illustrated that the ZnCPI liposome (pH 4.6) had effective antitumor activity with laser irradiation, without any adverse reactions.[59]

Visudyne®, containing the photosensitizer verteporfin known as a benzoporphyrin derivative monoacid ring A, is a liposomal photosensitizer approved for clinical application. Visudyne® was developed by Novartis Ophthalmicis (Switzerland) and QLT (Canada).[60] It was approved by the FDA in 2000 to treat age-related macular degeneration,[61] and in 2001 to treat pathological myopia.[62,63] Due to a very low solubility, verteporfin is formulated into a liposome consisting mainly of egg phosphatidylglycerol, dimyristoylphosphatidylcholine and two antioxidants of butylated hydroxytoluene and ascorbyl palmitate. The liposomal formulation of porphyrins belongs to the third generation of photosensitizers of PDT and appears to be one of the most promising photosensitizers. Foslip® is a liposomal photosensitizer approved for clinical application, which contains 5,10,15,20-tetra(*m*-hydroxyphenyl)chlorin (*m*-THPC) encapsulated into dipalmitoyl phosphatidylcholine/dipalmitoyl phosphatidylglycerol (DPPC/DPPG) liposomes in a ratio of 9 : 1.[64] Compared to Foscan®, using Foslip® as a photosensitizer, PDT treatment could result in a higher efficacy, reduced damage to surrounding healthy tissue and a shortened hospital stay.[65,66] Foscan® is a clinically approved photosensitizer that is widely used in Europe for the PDT of head and neck and other cancers.[67–69] de Visscher *et al.* demonstrated that Foslip® exhibited higher bioavailability and tumour selectivity than Foscan® by comparing their

fluorescence kinetic profiles.[70] Vascular *m*-THPC fluorescence increased for Foslip® but decreased for Foscan®.

5-Aminolevulinic acid (ALA) has been widely used for PDT due to its capability to convert into the endogenous photosensitizer protoporphyrin IX. A major drawback of ALA is its low bioavailability as a result of the poor penetration of ALA into tissues. To resolve this problem, ALA was loaded into liposomes with a molar ratio of PE phosphatidyl ethanoamine (PE)/cholesterol/sodium stearate at 2 : 1 : 2.5, which represented the best condition to achieve a high entrapment efficiency of about 29%. According to the release rate and skin penetration of the ALA liposome *in vitro*, the potential enhancement of penetration must involve sodium stearate concurrently with PE and cholesterol to achieve a positive effect.[71] Likewise, the inclusion of ALA esters, especially of ALA hexyl esters, appeared to result in a higher stability upon dilution with cell culture medium. During PDT treatments, image guidance is essential for precise and safe light delivery to the targeting site, thus improving the therapeutic effectiveness.[72] Dai *et al.* fabricated theranostic porphyrin dyad nanoparticles (TPD NPs) for magnetic resonance imaging (MRI)-guided PDT cancer therapy by forming liposome-like nanoparticles with the lipid of metal-free porphyrin, followed by conjugating a Mn–porphyrin (Fig. 3). The inner metal-free porphyrin functions as a photosensitizer for PDT, while the outer Mn–porphyrin serves as an MRI contrast agent. The covalent attachment of porphyrins to TPD NPs avoids premature release during systemic circulation. In addition, TPD NPs (~60 nm) could passively accumulate in tumours and be avidly taken up by tumour cells. After a 24 h intravenous injection of TPD NPs, MRI images showed that the whole tumour area remained much brighter than the surrounding healthy tissue, allowing researchers to guide the laser light to the desired tumour site for photodynamic ablation.[73] A photosensitizer, 3-vinyl-3-[1-(hexyoxy)ethyl]pyropheophorbide (HPPH), was conjugated to an MRI contrast agent, Gd(III)-aminobenzyl-diethylenetriaminepentaacetic acid (DTPA), *via* a tris(polyethylene glycol)monomethyl-ether linkage, followed by encapsulating it into liposomes. MRI imaging showed that this conjugate could enhance tumour localisation by a 10-fold lower dose than Magnevist® while maintaining its PDT efficacy.[74,75]

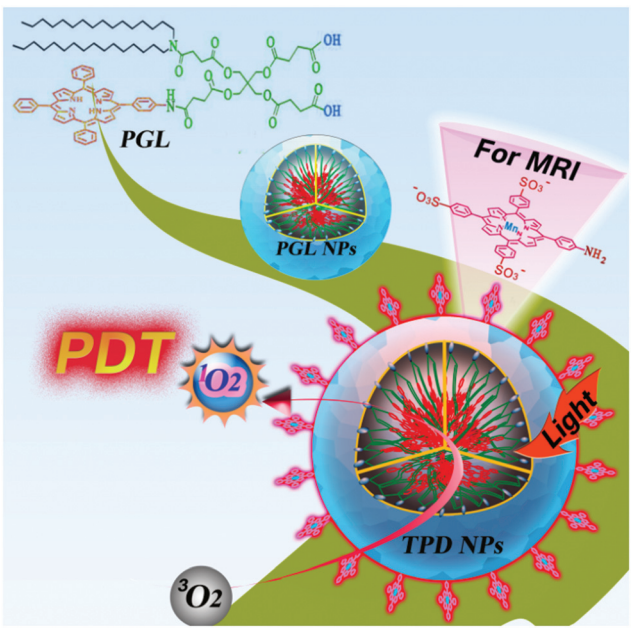

Fig. 3 Schematic illustration for the formation of theranostic porphyrin dyad nanoparticles. Reprinted with permission from ref. 73. Copyright © 2014 Elsevier Ltd.

The potential limitations of conventional liposomes are their short circulatory half-life and insufficient tumour selectivity. Fospeg® is another liposomal formulation of *m*-THPC that has been designed to improve the stability and prolong the half-life of *m*-THPC by coating with PEG.[76,77] Many studies have demonstrated that PEGylated liposomes (Fospeg®) are promising nanocarriers for the delivery of photosensitizers for PDT due to their reduced dark cytotoxicity and increased therapeutic efficacy. Active targeting is often used to enhance tumour-selective accumulation by site-directed retention *via* target binding and thus can improve the photodynamic effect through cellular internalisation of the porphyrin-loaded liposome. In this way, the undesired side-effects related to non-specific photosensitizer accumulation may be minimized. The pentapeptide (APRPG) is often used to target angiogenic endothelial cells. It was reported that APRPG-conjugated liposomal benzoporphyrin derivative monoacid ring A (BPD-MA) exhibited strong suppression of tumour growth compared to tumors targeted with a non-APRPG NPS.[78] By loading 5,10,15,20-tetraphenylporphyrin into polymeric micelles, followed by modification with tumour specific monoclonal antibody 2C5 (mAb 2C5) against murine Lewis lung carcinoma, increased drug accumulation in the tumour was achieved, indicating the obvious anti-tumour activity of this modified formulation due to improvement of the target cell specificity.[79] The photosensitizer of amphiphilic hypericin was loaded into transferrin-modified liposomes as theranostic agents for fluorescence/photoacoustic imaging and cancer PDT.[80] Transferrin was used as the tumour-seeking molecule, because many tumour cells overexpress transferrin receptors on their surface as a result of their elevated request for iron. The spectroscopic features of hypericin indicated the successful insertion of hypericin into dipalmitoyl phosphatidylcholine liposomes.[81] However, targeting hypericin by transferrin-conjugated PEG-liposomes did not significantly favour the photocytotoxicity and the intracellular accumulation of hypericin, in comparison with non-targeted PEG-liposomes or free hypericin, due to the limited stability of the embedding of the photosensitizer in the liposomal membrane. Despite their proven efficiency as a targeting carrier system, transferrin-conjugated PEG-liposomes appear less effective in targeting hypericin to tumour cells due to the amount of hypericin leaking out of the PEG-liposomes.[80] Therefore, there is a pressing need to make further efforts to improve the stability of porphyrin-loaded liposomes.

Cerasomal porphyrin for the photodynamic theranostics of cancer

Although liposomes have achieved a lot of success as a delivery system of porphyrins, they still have not attained their full potential because of the insufficient chemical and physical stability,[82] leading to a short shelf-life and their rapid clearance from the blood circulation, often before reaching their target. A PEG coating of liposomes has been proven to prolong blood circulation.[83] However, PEGylated liposomes have been reported to cause skin toxicity generally known as "Hand-Foot syndrome"[84,85] and an accelerated blood clearance (ABC) phenomenon due to the formation of anti-PEG IgM. In addition, the existence of large PEG molecules surrounding the liposomes can reduce the interactions between the liposomes and cells and block the entrance of liposomes into the cancerous tissue.[86]

To overcome the general problems associated with current liposome technology, a new type of liposomal nanohybrid cerasome was developed. Cerasomes are constructed by the direct dispersion of lipidic organoalkoxysilane in an aqueous solution using vortex-mixing, resulting in the generation of multi-lamellar vesicles in the range of sub-micrometres *via in situ* sol–gel reactions ($Si–OCH_3CH_2 + H_2O \rightarrow Si–OH + CH_3CH_2OH$ followed by $2Si–OH \rightarrow Si–O–Si + H_2O$) and a subsequent self-assembly process.[87] Upon ultrasonication with a probe-type sonicator above the phase transition temperature of the lipids, the obtained multi-lamellar vesicles converted into single uni-lamellar vesicles less than 200 nm in a diameter. Cerasomes are similar to traditional liposomes and are spherical vesicles with a lipid bilayer membrane around 4 nm in thickness. An atomic layer of inorganic polyorganosiloxane networks spontaneously forms around the liposomal bilayer surface through silanol condensation. There is no need to introduce cholesterol during the fabrication of cerasomes, while conventional liposomes often include cholesterol as a constituent to improve the rigidity and stability of the phospholipid bilayer membrane.

The siloxane coating offers cerasomes with significantly higher mechanical stability and heat resistance than conventional liposomes, and the liposomal bilayer structure of cerasomes reduces the overall rigidity and density greatly in comparison with silica nanoparticles. The size of liposomes is often observed to increase during storage because of their aggregation or fusion. On the contrary, cerasomes can be stored in an aqueous solution at 4 °C for several months with almost no change in size.[84] Moreover, cerasomes exhibit high stability upon surfactant solubilisation and acid treatment.[87] Cerasomes show better biocompatibility than silica nanoparticles because of the introduction of the liposomal architecture into cerasomes. Cerasomes combine the advantages of both liposomes and silica nanoparticles but overcome their disadvantages, thus cerasomes are considered ideal drug delivery systems.[88,89]

Because of their flexibility to accommodate porphyrins, liposomes are generally used to encapsulate porphyrins to improve the efficacy and safety of PDT.[90] Nevertheless, loaded porphyrins are often observed to release into the bloodstream because lipid exchange between the liposomes and lipoproteins can lead to an irreversible disintegration of the liposome. This is different from conventional chemotherapy, where the photosensitizer release is not an essential prerequisite of a successful PDT action because this premature release can lead to reduction in PDT efficacy.[91] To resolve this problem, Dai *et al.* designed and fabricated a novel cerasomal porphyrin *via* a sol–gel reaction and self-assembly process using a porphyrin–organoalkoxysilylated lipid conjugate (PORSIL), which consisted of dual triethoxysilyl heads, a hydrophobic double-chain segment, a porphyrin moiety and a connector unit among them (Fig. 4). The resulting cerasomal porphyrin had a diameter around 70 ± 13 nm. The drug loading content was evaluated to be 33.46%, remarkably higher than the traditional liposomal porphyrins (usually less than 10%). Moreover, no premature release of porphyrin photosensitizer was observed during systemic circulation due to the covalent attachment of porphyrin molecules into cerasomes.[92]

After dissolution in an organic solvent, both Soret and Q bands of the porphyrin–organoalkoxysilylated lipid conjugate of PORSIL showed a 3 nm red-shift attributed to the orderly arranging mode of the porphyrin moiety in the lipid bilayer. The shape of the absorption spectrum of the cerasomal porphyrin is far more similar to that of the solution-phase PORSIL lipid. This demonstrated that no phorphyrin aggregation was generated in the cerasome nanoparticles. In such porphyrin-loaded cerasomes, each porphyrin moiety is separated by a double-alkyl chain, which sterically hinders the porphyrin moieties that approach each other.[92] This is very efficient for fabricating photodynamic cerasomes by encapsulating a porphyrin

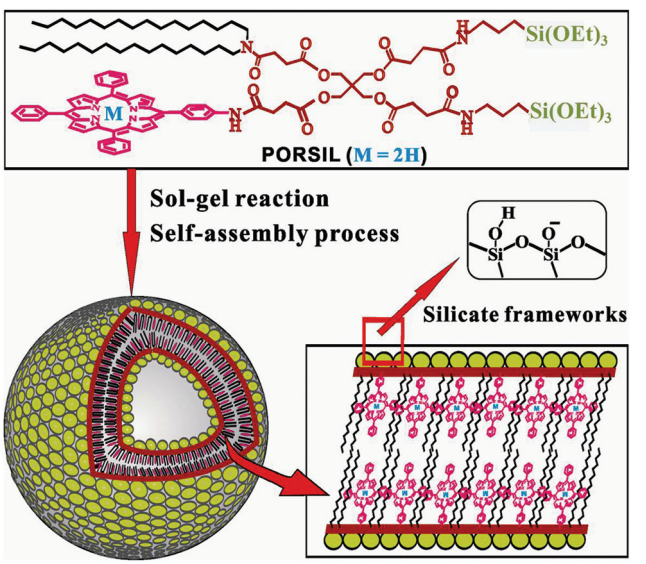

Fig. 4 Schematic illustration for the formation of porphyrin-conjugated cerasome from a PORSIL lipid. Reprinted with permission from ref. 92. Copyright ©2011 Wiley.

photosensitizer without causing any aggregation of porphyrin molecules. The existence of the double-alkyl chains can prevent fluorescence self-quenching in cerasomal porphyrins, thus permitting its use as a powerful tool for *in vivo* imaging.

The blood circulation dynamics of the cerasomal porphyrin was studied with liposomal porphyrin as the control. The liposomal porphyrin showed rapid clearance kinetics and its blood fluorescence intensity reduced to 30% after intravenous injection after 6 h and almost disappeared at 24 h. In contrast, the cerasomal porphyrin exhibited dramatically prolonged and slow clearance kinetics and remained at 66.5% blood fluorescence intensity at 24 h. This illustrated clearly that the cerasomal porphyrin had a long circulation time even with no PEGylation.

The uptake of cerasomes by cells was found to be a concentration-, time-, and energy-dependent process and occurred probably through a process of clathrin-mediated endocytosis. The porphyrin-conjugated cerasomes were seen to be highly fluorescent as red spots distributed in the cytoplasm by using confocal laser scanning microscopy. Moreover, the capability of porphyrin to produce $^1O_2$ by photosensitization was enhanced greatly, even at an extremely high number of porphyrins due to the conjugation to cerasomes. An obvious phototoxic effect on the cancer cells was observed after treatment with the porphyrin-conjugated cerasomes in combination with irradiation of the light (400–700 nm). Furthermore, no apparent dark toxicity was observed. The ability to load chemotherapeutic drugs into the internal aqueous core of the porphyrin-conjugated cerasomes makes it possible to fabricate a drug-carrier system for the synergistic combination of chemotherapy and PDT for the treatment of cancer. Therefore, the dual function nature of the cerasomal porphyrin would definitely play a key role in future clinical photodynamic theranostics.

Porphysomes for cancer theranotics

Recently, Zheng's group reported another type of liposome-like porphyrin-loaded nanoparticles (termed porphysomes) with good biocompatibility and degradability, high drug loading content, high absorption coefficiency and structure-dependent fluorescence quenching (Fig. 5).[93,94] The porphysomes (100 nm) were supramolecularly self-assembled in aqueous media with a lipidic porphyrin synthesized by an acylation reaction between lysophosphatidylcholine and pyropheophorbide. TEM micrographs showed that the porphysomes consisted of two separate monolayers with a 2 nm gap.[94] The porphysomes exhibit good stability and can be stored for months in aqueous media, but they are susceptible to enzymatic degradation. The vesicular structure of the porphysome was disrupted upon incubation with lipase or detergents.[94] Like chlorophyll, its main material of pyropheophorbide can be enzymatically cleaved into colourless pyrroles in the presence of peroxidase or hydrogen peroxide.[95] By monitoring the absorbance loss of porphysomes, Lovell *et al.* proved the efficient degradation of pyropheophorbide and porphysomes by peroxidase, even at extremely high concentrations (1 g kg^{-1} injected dose).[94,96] The ability to use porphysomes as a

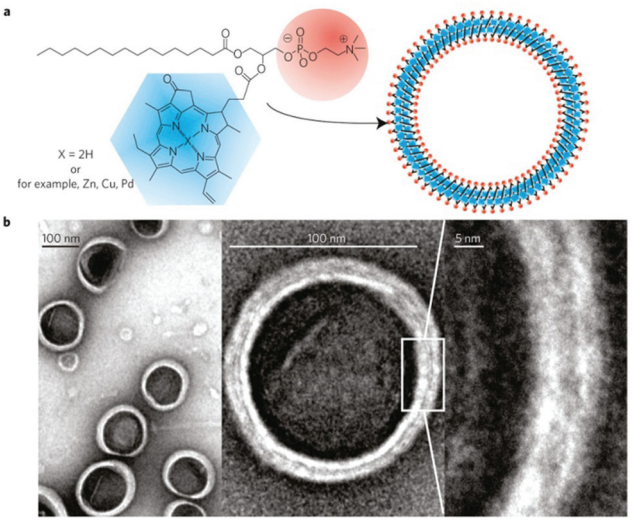

Fig. 5 Porphysomes are optically active nanovesicles formed from porphyrin bilayers. a, Schematic representation of a pyropheophorbide–lipid porphysome. b, Electron micrographs of negatively stained porphysomes (5% PEG–lipid, 95% pyropheophorbide–lipid). Reprinted with permission from ref. 94. Copyright © 2011 Macmillan Publishers Limited.

delivery system was also investigated.[94] By using the ammonium sulphate gradient method and incorporating 50% cholesterol to enhance the drug loading, doxorubicin was encapsulated into the porphysome core with 90% loading efficiency,[94] indicating that porphysome can act as a theranostic platform. The drug-loaded porphysomes maintained a self-quenching porphyrin bilayer.

Two absorption peaks were observed at 400 nm and 680 nm in the aqueous dispersion of porphysomes. Using bacteriochlorophyll analogue as subunits, red-shifted porphysomes (760 nm) were fabricated. By chelating metal ions into the lipidic porphyrin, the absorption peaks of porphysomes shifted to 440 nm and 670 nm, indicating the formation of metal-chelating bilayers in the porphysomes. Easy alteration of the photochemistry of the porphysomes provides a possibility to adjust the operating wavelengths to match the wavelengths of given laser sources.

The biocompatibility of porphysomes was evaluated. After treatment with a high dose (1000 mg kg^{-1}) of porphysomes for 2 weeks, mice were healthy with a normal hepatic function. The unaffected red blood cell counts and attributes suggested that the porphysome did not with the physiological regulation of endogenous porphyrin. The porphysomes had no effect on the white blood cell count, indicating no immunogenicity. No apparent changes were observed from histopathological examination of tissue slices such as heart, liver, spleen, lung and kidney, which were collected and stained with haematoxylin and eosin (H&E). All these results demonstrated the good biocompatibility and non-toxicity of porphysomes, which are required for *in vivo* biomedical applications.

While porphyrins are known to interact with light to generate fluorescence and singlet oxygen, the high packing density

of porphyrins within these nanovesicles (>80 000 porphyrins per porphysome) expanded the use of porphyrins for thermal-based therapy and imaging applications.[93] Porphysomes are highly self-quenched and exhibit highly efficient energy conversion from light into heat, which is comparable to photothermally active gold nanostructures. A photoacoustic signal is known to be generated by thermal expansion. Zheng's group discovered that porphysomes produced photoacoustic signals, which were proportional to the concentrations of porphysomes and detectable as low as 25 pM. Upon the addition of a detergent to a solution of porphysomes, the photoacoustic signal decreased six-fold due to disruption of the porphysome structure. This indicated that the photoacoustic behaviour of porphysomes depend on their self-quenching property. Then, Lovell *et al.* tested the ability of porphysomes to operate as photoacoustic contrast agents *in vivo*. After an intradermal injection of porphysome for 15 minutes, the local lymphatic system of rats was clearly seen by photoacoustic imaging, as the porphysomes drained to the lymph vessels and nodes and produced strong photoacoustic signals. Thus, porphysomes can be used as contrast agents to visualize the first draining lymph node, the in-flowing lymph vessel and surrounding lymph vessels by photoacoustic imaging.[94]

The capability to use porphysomes for photothermal ablation of tumours was investigated. It was found that the incorporation of 30 molar% of cholesterol into porphysomes was beneficial for biodistribution after the intravenous injection of porphysomes. Compared to standard porphysomes, the tumour tissue (KB tumour-bearing mice) had more accumulation than normal tissues, including the liver, spleen and kidneys. After 24 h intravenous injection of the porphysomes, the tumour was irradiated with laser light for 1 min. The tumour temperature was monitored by a thermal camera. It was seen that the tumour temperature increased to 60 °C rapidly, 20 °C higher than the PBS injected mice as control. Following the treatment with porphysomes combined with laser irradiation, mice developed eschars on the tumours and the eschars healed after two weeks. On the contrary, no eschars were developed in the laser-alone and porphysome-alone control groups and the size of tumours increased rapidly.[94] The porphysomes were further used to destroy both hyperoxic and hypoxic tumours. Moreover, the destruction of tumours was demonstrated by photothermal heating and not by a photodynamic effect due to the self-quenching of the porphyrin within the porphysome nanostructure.[97]

Taking advantage of the structure-dependent self-quenching property of porphysomes, Cui *et al.* demonstrated activatable PDT by targeting the porphysomes to the folate receptor, overexpressed in many cancer cell lines.[98] A 1 mol% folate-PEG-lipid was introduced into the porphysomes for specific tumour uptake. It was found that fluorescence was restored and singlet-oxygen was produced to kill the tumor cells upon uptake by KB cells (folate positive cells).[99] After systemic administration for 15 min, a low fluorescence signal was noted due to the self-quenching of porphysomes. Nevertheless, the fluorescence became strong in the tumour after two days because the porphysomes were dequenched in the tumour.[94] When detergent-disrupted porphysomes were injected, the porphysome quenching was remarkably enhanced, and hence a higher fluorescence was observed in the tumor. Therefore, porphysomes can act intrinsically as a bimodal contrast agent to enhance both photoacoustic and fluorescence imaging.

The feature of the porphyrin to chelate metals offers another capability to utilize the high porphyrin content obtained with porphysomes for whole body imaging. Porphysomes could be radiolabelled with copper-64 with a specific activity of 2800 Ci per μmol per nanoparticle.[99] Radiolabelled porphysomes were used as a dual imaging agent for PET and for fluorescence imaging in an orthotopic prostate cancer model to clearly distinguish the prostate tumour from surrounding organs, including the bladder and prostate.[100] In particular, a small prostate cancer bone metastasis (<2 mm) was identified, offering the potential to monitor tumour recurrence and response to treatment.

Pyropheophorbide–lipid was further used to form microbubbles with a porphyrin shell encapsulating a perfluoropropane gas.[101] The porphyrin-lipid offered a photoacoustic function to the microbubble, leading to a multimodal ultrasonic/photoacoustic microbubble. Such multimodal microbubbles have promising use in drug delivery and as optical imaging agents, potentially overcoming the resolution limitations associated with mere ultrasound imaging. Instead of releasing drugs by expanding microbubbles as reported previously, Zheng *et al.* imploded these ultrasonic/photoacoustic/fluorescent multimodal microbubbles into nanoparticles with diameters ranging from 5 nm to 500 nm using ultrasound. Due to their small size, the resulting nanoparticles retain their fluorescent and photoacoustic properties, but lose their acoustic reflectivity, and thus are expected to penetrate tissues more easily. Their ultrasound imaging capability gives image-based guidance to the delivery of drugs, and the fluorescence imaging allows for evaluating the concentration of the drug reaching the target tissue.[102]

Conclusions

A variety of porphyrins have been developed as PDT photosensitizing agents but few of them have been successfully employed in clinical trials due to their low aqueous solubility and poor selectivity to tumorous tissue. However, loading porphyrins into nanoparticles can make hydrophobic porphyrins soluble in water and passively target tumour tissue. In addition, by conjugating specific targeting moieties to the porphyrin nanoparticle surface, selective accumulation can be further achieved.

Nowadays, various imaging modalities (*e.g.* MRI, CT, and PET) have been widely utilized in PDT planning and assessment. It is expected that multimodality imaging combined with PDT will gain the most use ultimately due to the capability to obtain both structural and functional images. Therefore, a theranostic agent for both multimodal imaging and the

PDT of cancer urgently needs to be developed. As a multifunctional nanoplatform, porphyrin-loaded nanoparticles offer theranostic advantages because they can be further used to load the other imaging contrast agents (*e.g.* radionuclides, quantum dots, Gd complex, Fe_3O_4 and gold nanoparticles) for PET, fluorescence, MRI, CT and photoacoustic imaging. Moreover, the own fluorescence of the porphyrin nanoparticles can be used as an imaging signal. In addition, the other therapeutic agents (*e.g.* radionuclides, doxorubicin, paclitaxel, siRNA, DNA) can be introduced into porphyrin-loaded nanoparticles for radiotherapy, chemotherapy, photothermal therapy, photodynamic therapy, gene therapy and combined therapy.

The multimodality imaging functionalization of therapeutic porphyrin nanoparticles is of particular interest for the personalized monitoring of *in vivo* tumor targeting and the pharmacokinetics of porphyrin for predicting the therapy outcome. In combination of the advantageous information from each imaging modality, we can better understand the prognosis-associated disease status. Therefore, undoubtedly the multifunctional nature of the porphyrin-loaded nanoparticles will play an important role in future clinical photodynamic theranostics for non-invasive imaging diagnosis, real-time imaging guidance and remote-controlled therapeutics, especially imaging-guided therapeutics. Nonetheless, it is not to say that this nanoplatform has no drawbacks. The porphyrin-loaded nanoparticles are still in the initial stages of clinical trials and some basic aspects remain to be studied in more detail. It is necessary to address some issues concerning transitional medicine of such porphyrin-loaded nanoparticles, including transport barriers, drug uptake, distribution hurdles, and their long-term effects. The deep exploitation of such novel nanoparticles may gain the wide interests of clinicians.

Acknowledgements

This study was financially supported by the State Key Program of National Natural Science of China (Grant No. 81230036), National Natural Science Foundation of China (no. 21273014 and 81201186), National Natural Science Foundation for Distinguished Young Scholars (no. 81225011) and China Postdoctoral Science Foundation (2013M530014).

References

1 A. Jemal, F. Bray, M. M. Center, J. Ferlay, E. Ward and D. Forman, *CA-Cancer J. Clin.*, 2011, **61**, 69–90.
2 G. K. Dy and A. A. Adjei, *CA-Cancer J. Clin.*, 2013, **63**, 249–279.
3 X. Yue and Z. Dai, *Adv. Colloid Interface Sci.*, 2014, **207**, 32–42.
4 R. Liu, L. Jing, D. Peng, Y. Li, J. Tian and Z. Dai, *Theranostics*, 2015, **5**, 1144–1153.
5 C. Guo, Y. Jin and Z. Dai, *Bioconjugate Chem.*, 2014, **25**, 840–854.
6 L. Jing, X. Liang, X. Li, L. Lin, Y. Yang, X. Yue and Z. Dai, *Theranostics*, 2014, **4**, 858–871.
7 Y. Li, S. Zheng, X. Liang, Y. Jin, Y. Wu, H. Bai, R. Liu, Z. Dai, Z. Liang and T. Shi, *Bioconjugate Chem.*, 2014, **25**, 2055–2066.
8 G. Fu, W. Liu, Y. Li, Y. Jin, L. Jiang, X. Liang, S. Feng and Z. Dai, *Bioconjugate Chem.*, 2014, **25**, 1655–1663.
9 H. Ke, J. Wang, S. Tong, Y. Jin, S. Wang, E. Qu, G. Bao and Z. Dai, *Theranostics*, 2014, **4**, 12–23.
10 E. Paszko, C. Ehrhardt, M. O. Senge, D. P. Kelleher and J. V. Reynolds, *Photodiagn. Photodyn. Ther.*, 2011, **8**, 14–29.
11 M. G. Vicente, *Curr. Med. Chem.: Anti-Cancer Agents*, 2001, **1**, 175–194.
12 X.-a. Zhang, K. S. Lovejoy, A. Jasanoff and S. J. Lippard, *Proc. Natl. Acad. Sci. U. S. A.*, 2007, **104**, 10780–10785.
13 K. Hachimine, H. Shibaguchi, M. Kuroki, H. Yamada, T. Kinugasa, Y. Nakae, R. Asano, I. Sakata, Y. Yamashita, T. Shirakusa and M. Kuroki, *Cancer Sci.*, 2007, **98**, 916–920.
14 M. Miura, D. Gabel, G. Oenbrink and R. G. Fairchild, *Tetrahedron Lett.*, 1990, **31**, 2247–2250.
15 W. Chen and J. Zhang, *J. Nanosci. Nanotechnol.*, 2006, **6**, 1159–1166(1158).
16 B. Chen, B. W. Pogue and T. Hasan, *Expert Opin. Drug Delivery*, 2005, **2**, 477–487.
17 G. Obaid, I. Chambrier, M. J. Cook and D. A. Russell, *Photochem. Photobiol. Sci.*, 2015, **14**, 737–747.
18 S. H. Voon, L. V. Kiew, H. B. Lee, S. H. Lim, M. I. Noordin, A. Kamkaew, K. Burgess and L. Y. Chung, *Small*, 2014, **10**, 4993–5013.
19 L. Cui, Q. Lin, C. S. Jin, W. Jiang, H. Huang, L. Ding, N. Muhanna, J. C. Irish, F. Wang, J. Chen and G. Zheng, *ACS Nano*, 2015, **9**, 4484–4495.
20 L. B. Josefsen and R. W. Boyle, *Met.-Based Drugs*, 2008, **2008**, 276109.
21 M. Ethirajan, Y. Chen, P. Joshi and R. K. Pandey, *Chem. Soc. Rev.*, 2011, **40**, 340–362.
22 J. F. Lovell, T. W. B. Liu, C. Juan and Z. Gang, *Chem. Rev.*, 2010, **110**, 2839–2857.
23 R. Allison, K. Moghissi, G. Downie and K. Dixon, *Photodiagn. Photodyn. Ther.*, 2011, **8**, 231–239.
24 K. Moghissi, *Curr. Opin. Pulm. Med.*, 2004, **10**, 256–260.
25 J. P. Celli, B. Q. Spring, R. Imran, C. L. Evans, K. S. Samkoe, V. Sarika, B. W. Pogue and T. Hasan, *Chem. Rev.*, 2010, **110**, 2795–2838.
26 M. D. Glidden, J. P. Celli, I. Massodi, I. Rizvi, B. W. Pogue and T. Hasan, *Theranostics*, 2012, **2**, 827–839.
27 S. Mitra, O. Mironov and T. H. Foster, *Theranostics*, 2012, **2**, 840–849.
28 N. Yumita, Y. Iwase, K. Nishi, H. Komatsu, K. Takeda, K. Onodera, T. Fukai, T. Ikeda, S. Umemura, K. Okudaira and Y. Momose, *Theranostics*, 2012, **2**, 880–888.
29 G. Zheng, J. Chen, K. Stefflova, M. Jarvi, H. Li and B. C. Wilson, *Natl. Acad. Sci. USA*, 2007, **104**, 8989–8994.

30 G. Li, A. Slansky, M. P. Dobhal, L. N. Goswami, A. Graham, Y. Chen, P. Kanter, R. A. Alberico, J. Spernyak, J. Morgan, R. Mazurchuk, A. Oseroff, Z. Grossman and R. K. Pandey, *Bioconjugate Chem.*, 2005, **16**, 32–42.
31 J. Shi, T. W. B. Liu, J. Chen, D. Green, D. Jaffray, B. C. Wilson, F. Wang and G. Zheng, *Theranostics*, 2011, **1**, 363–370.
32 G. Firnau, D. Maass, B. C. Wilson and W. P. Jeeves, *Prog. Clin. Biol. Res.*, 1984, **170**, 629–636.
33 T. W. B. Liu, J. Chen, L. Burgess, W. Cao, J. Shi, B. C. Wilson and G. Zheng, *Theranostics*, 2011, **1**, 354–362.
34 R. Allison, K. Moghissi, G. Downie and K. Dixon, *Photodiagn. Photodyn. Ther.*, 2011, **8**, 231–239.
35 B. A. Teicher, *Drug Resist. Updates*, 2000, **3**, 67–73.
36 G. W. Sledge and K. D. Miller, *Eur. J. Cancer*, 2003, **39**, 1668–1675.
37 R. Indrajit, T. Y. Ohulchanskyy, H. E. Pudavar, E. J. Bergey, A. R. Oseroff, M. Janet, T. J. Dougherty and P. N. Prasad, *J. Am. Chem. Soc.*, 2003, **125**, 7860–7865.
38 P. Huang, J. Lin, X. Wang, Z. Wang, C. Zhang, M. He, K. Wang, F. Chen, Z. Li, G. Shen, D. Cui and X. Chen, *Adv. Mater.*, 2012, **24**, 5104–5110.
39 W. Chen and J. Zhang, *J. Nanosci. Nanotechnol.*, 2006, **6**, 1159–1166.
40 H. Gu, K. Xu, Z. Yang, C. K. Chang and B. Xu, *Chem. Commun.*, 2005, 4270–4272.
41 M. Gautherie, C. Streffer, P. Vaupe and G. M. Hahn, *Biological Basis of Oncologic Thermotherapy*, Springer, New York, 1990.
42 Y. N. Konan, R. Gurny and E. Allémann, *J. Photochem. Photobiol., B*, 2002, **66**, 89–106.
43 Y. N. Konan, M. R. Berton and E. Allemann, *Eur. J. Pharm. Sci.*, 2003, **18**, 241–249.
44 Y. N. Konan, R. Cerny, J. Favet, M. Berton, R. Gurny and E. Allémann, *Eur. J. Pharm. Biopharm.*, 2003, **55**, 115–124.
45 A. Vargas, B. Pegaz, E. Debefve, Y. N. Konan, N. Lange, J. P. Ballini, d. B. H. Van, R. Gurny and F. Delie, *Int. J. Pharm.*, 2004, **286**, 131–145.
46 Y. N. Konan, R. Boch, R. Gurny and E. Allemann, *J. Controlled Release*, 2005, **103**, 83–91.
47 L. Jing, X. Liang, X. Li, L. Lin, Y. Yang, X. Yue and Z. Dai, *Theranostics*, 2014, **4**, 858–871.
48 B. Li, E. H. Moriyama, F. Li, M. T. Jarvi, C. Allen and B. C. Wilson, *Photochem. Photobiol.*, 2007, **83**, 1505–1512.
49 C. Kojima, Y. Toi, A. Harada and K. Kono, *Bioconjugate Chem.*, 2007, **18**, 663–670.
50 J. Lin, S. Wang, P. Huang, Z. Wang, S. Chen, G. Niu, W. Li, J. He, D. Cui, G. Lu, X. Chen and Z. Nie, *ACS Nano*, 2013, **7**, 5320–5329.
51 P. Huang, C. Xu, J. Lin, C. Wang, X. Wang, C. Zhang, X. Zhou, S. Guo and D. Cui, *Theranostics*, 2011, **1**, 240–250.
52 H. Benachour, A. Sève, T. Bastogne, C. Frochot, R. Vanderesse, J. Jasniewski, I. Miladi, C. Billotey, O. Tillement, F. Lux and M. Barberi-Heyob, *Theranostics*, 2012, **2**, 889–904.
53 M. J. Shieh, C. L. Peng, W. L. Chiang, C. H. Wang, C. Y. Hsu, S. J. Wang and P. S. Lai, *Mol. Pharmaceutics*, 2010, **7**, 1244–1253.
54 W. Li, W. Lu, Z. Fan, X. Zhu, A. Reed, B. Newton, Y. Zhang, S. Courtney, P. T. Tiyyagura, R. R. Ratcliff, S. Li, E. Butler, H. Yu, P. C. Ray and R. Gao, *J. Mater. Chem.*, 2012, **22**, 12701–12708.
55 J. Hu, Y. A. Tang, A. H. Elmenoufy, H. Xu, Z. Cheng and X. Yang, *Small*, 2015, **11**(44), 5860–5887.
56 F. Jiang, L. Lilge, G. Joseph, Y. Li, M. D. Wilson and M. Chopp, *Lasers Surg. Med.*, 1998, **22**, 74–80.
57 C. Milanesi, F. Sorgato and G. Jori, *Int. J. Radiat. Biol.*, 1989, **55**, 59–69.
58 F. Ricchelli, S. Gobbo, G. Jori, G. Moreno, F. Vinzens and C. Salet, *Photochem. Photobiol.*, 1993, **58**, 53–58.
59 Y. Sadzuka, F. Iwasaki, I. K. Horiuchi, T. Hirano, H. Ozawa, N. Kanayama and T. Sonobe, *Int. J. Pharm.*, 2007, **338**, 306–309.
60 Y. N. Konan, R. Gurny and E. Allémann, *J. Photochem. Photobiol., B*, 2002, **66**, 89–106.
61 N. M. Bressler, *Arch. Ophthalmol.*, 1999, **117**, 1329–1345.
62 J. G. Christie and U. B. Kompella, *Drug Discovery today*, 2008, **13**, 124–134.
63 B. Pegaz, E. Debefve, F. Borle, J. P. Ballini, H. V. D. Bergh and Y. N. Konan, *J. Photochem. Photobiol., B*, 2005, **80**, 19–27.
64 J. Buchholz, B. Kaser-Hotz, T. Khan, C. Rohrer Bley, K. Melzer, R. A. Schwendener, M. Roos and H. Walt, *Clini. Cancer Res.*, 2005, **11**, 7538–7544.
65 H. Lassalle, D. Dumas, S. Grafe, M. A. D'Hallewin, F. Guillemin and L. Bezdetnaya, *J. Controlled Release*, 2009, **134**, 118–124.
66 T. Kiesslich, J. Berlanda, K. Plaetzer, B. Krammer and F. Berr, *Photochem. Photobiol. Sci.*, 2007, **6**, 619–627.
67 M. Sadasivam, P. Avci, G. K. Gupta, S. Lakshmanan, R. Chandran, Y. Y. Huang, R. Kumar and M. R. Hamblin, *Eur. J. Nanomed.*, 2013, **5**, 115–129.
68 T. Kiesslich, J. Berlanda, K. Plaetzer, B. Krammer and F. Berr, *Photochem. Photobiol. Sci.*, 2007, **6**, 619–627.
69 B. Pegaz, E. Debefve, J. P. Ballini, G. Wagnières, S. Spaniol, V. Albrecht, D. V. Scheglmann, N. E. Nifantiev, H. V. D. Bergh and Y. N. Konan-Kouakou, *J. Pharm. Sci.*, 2006, **28**, 134–140.
70 S. A. H. J. D. Visscher, H. S. D. Bruijn, A. Amelink, H. J. C. M. Sterenborg, D. J. Robinson, J. L. N. Roodenburg and M. J. H. Witjes, *Lasers Surg. Med.*, 2011, **43**, 528–536.
71 Y. P. Fang, P. C. Wu, Y. H. Tsai and Y. B. Huang, *J. Liposome Res.*, 2008, **18**, 31–45.
72 G. D. Venosa, L. Hermida, A. Batlle, H. Fukuda, M. V. Defain, L. Mamone, L. Rodriguez, A. Macrobert and A. Casas, *J. Photochem. Photobiol., B*, 2008, **92**, 1–9.
73 X. Liang, X. Li, L. Jing, X. Yue and Z. Dai, *Biomaterials*, 2014, **35**, 6379–6388.
74 M. Ethirajan, Y. Chen, P. Joshi and R. K. Pandey, *Chem. Soc. Rev.*, 2011, **40**, 340–362.

75 J. P. Celli, B. Q. Spring, I. Rizvi, C. L. Evans, K. S. Samkoe, S. Verma, B. W. Pogue and T. Hasan, *Chem. Rev.*, 2010, **110**, 2795–2838.
76 M. A. D'Hallewin, D. Kochetkov, V. B. Yan, M. D. Agnes Leroux, E. Werkmeister, D. Dumas, S. Gräfe, V. Zorin, M. D. François Guillemin and L. Bezdetnaya, *Lasers Surg. Med.*, 2008, **40**, 543–549.
77 V. Reshetov, V. Zorin, A. Siupa, M. A. D'Hallewin, F. Guillemin and L. Bezdetnaya, *Photochem. Photobiol.*, 2012, **88**, 1256–1264.
78 K. Ichikawa, T. Hikita, N. Maeda, S. Yonezawa, Y. Takeuchi, T. Asai, Y. Namba and N. Oku, *Biochim. Biophys. Acta*, 2005, **1669**, 69–74.
79 A. Roby, S. Erdogan and V. P. Torchilin, *Cancer Biol. Ther.*, 2007, **6**, 1136–1142.
80 A. S. Derycke and P. A. de Witte, *Int. J. Oncol.*, 2002, **20**, 181–187.
81 A. Losi, *Photochem. Photobiol.*, 1997, **65**, 791–801.
82 A. Puri, K. Loomis, B. Smith, J. H. Lee, A. Yavlovich, E. Heldman and R. Blumenthal, *Crit. Rev. Ther. Drug Carrier Syst.*, 2009, **26**, 523–580.
83 T. Allen, C. Hansen, F. Martin, C. Redemann and A. Yau-Young, *Biochim. Biophys. Acta*, 1991, **1066**, 29–36.
84 Z. Cao, Y. Ma, X. Yue, S. Li, Z. Dai and J. Kikuchi, *Chem. Commun.*, 2010, **46**, 5265–5267.
85 K. B. Gordon, A. Tajuddin, J. Guitart, T. M. Kuzel, L. R. Eramo and J. VonRoenn, *Cancer*, 1995, **75**, 2169–2173.
86 T. Ishida, M. Ichihara, X. Wang and H. Kiwada, *J. Controlled Release*, 2006, **115**, 243–250.
87 K. Katagiri, M. Hashizume, K. Ariga, T. Terashima and J.-i. Kikuchi, *Chem. – Eur. J.*, 2007, **13**, 5272–5281.
88 K. Matsui, S. Sando, T. Sera, Y. Aoyama, Y. Sasaki, T. Komatsu, T. Terashima and J. Kikuchi, *J. Am. Chem. Soc.*, 2006, **128**, 3114–3115.
89 X. Yue and Z. Dai, *Adv. Colloid Interface Sci.*, 2014, **207**, 32–42.
90 A. S. L. Derycke and P. A. M. de Witte, *Adv. Drug Delivery Rev.*, 2004, **56**, 17–30.
91 I. Roy, T. Y. Ohulchanskyy, H. E. Pudavar, E. J. Bergey, A. R. Oseroff, J. Morgan, T. J. Dougherty and P. N. Prasad, *J. Am. Chem. Soc.*, 2003, **125**, 7860–7865.
92 X. Liang, X. Li, X. Yue and Z. Dai, *Angew. Chem., Int. Ed.*, 2011, **50**, 11622–11627.
93 E. Huynh and G. Zheng, *Nano Today*, 2014, **9**, 212–222.
94 J. F. Lovell, C. S. Jin, E. Huynh, H. Jin, C. Kim, J. L. Rubinstein, W. C. Chan, W. Cao, L. V. Wang and G. Zheng, *Nat. Mater.*, 2011, **10**, 324–332.
95 Y. Suzuki, K. Tanabe and Y. Shioi, *J. Chromatogr. A*, 1999, **839**, 85–91.
96 J. F. Lovell, C. S. Jin, E. Huynh, T. D. MacDonald, W. Cao and G. Zheng, *Angew. Chem., Int. Ed.*, 2012, **51**, 2429–2433.
97 C. S. Jin, J. F. Lovell, J. Chen and G. Zheng, *ACS Nano*, 2013, **7**, 2541–2550.
98 C. S. Jin, L. Cui, F. Wang, J. Chen and G. Zheng, *Adv. Healthcare Mater.*, 2014, **3**, 1122–1122.
99 T. W. Liu, T. D. Macdonald, J. Shi, B. C. Wilson and G. Zheng, *Angew. Chem., Int. Ed.*, 2012, **51**, 13128–13131.
100 T. W. Liu, T. D. MacDonald, C. S. Jin, J. M. Gold, R. G. Bristow, B. C. Wilson and G. Zheng, *ACS Nano*, 2013, **7**, 4221–4232.
101 E. Huynh, J. F. Lovell, B. L. Helfield, M. Jeon, C. Kim, D. E. Goertz, B. C. Wilson and G. Zheng, *J. Am. Chem. Soc.*, 2012, **134**, 16464–16467.
102 E. Huynh, B. Y. C. Leung, B. L. Helfield, M. Shakiba, J. Gandier, C. S. Jin, E. R. Master, B. C. Wilson, D. E. Goertz and G. Zheng, *Nat. Nanotechnol.*, 2015, **10**, 325–332.